Near Minimax Robust Control of Flexible Structures

Marco Muenchhof — Graduate Student
Tarunraj Singh — Associate Professor
Department of Mechanical and Aerospace Engineering
SUNY at Buffalo, Buffalo, New York, 14260

Add TU Darmstadt to my title

Abstract

This paper presents an approach to calculate prefilters that are insensitive to parameter deviations. The cost function chosen for this approach is the magnitude of the time-delay filter transfer function. By approximating the cost function with a polynomial, the effort of calculating minimax robust profiles can be reduced. The resulting control profiles yield a performance similar to the minimax robust controller. This is verified by the numerical results included in this paper.

1 Introduction

Numerous researchers have studied the problem of control of residual vibration of flexible structures. Since these residual vibrations can severely degrade the control performance, various approaches have been investigated aiming at a reduction in the undesired excitation of the oscillatory modes. This research is important for areas as diverse as maneuvering of large space structures [1], flexible arm robots [2], computer disk drives [3], and cranes [4].

One of the techniques proposed to cope with the aforementioned problem is based on an input prefiltering technique, which was first discussed by Smith [5] and which he termed *Posicast Control* . It is based on the superposition of a couple of delayed input sequences spaced such that the excitation of the oscillatory mode, which cannot be avoided during the maneuver, is counteracted. The performance of this controller was hampered by parametric uncertainties which could stem from modeling uncertainties or the exclusion of some modes from the system model. Despite these limitations, the results are still very promising, since it is possible to reach settling times faster than the period of the natural frequency of the system while warranting quiescent final states.

Different methods have been proposed to deal with the aforementioned model imprecisions. Singer and Seering [6] suggested an approach to design input shapers addressing the sensitivity of the posicast controllers with respect to damping ratio and natural frequency of the oscillatory mode. In order to robustify the time delay filter, they set the derivative of the constraint equation with respect to the natural frequency to zero. They also showed that desensitizing the controller with respect to the natural frequency also results in decreased sensitivity with respect to the damping ratio.

Singh and Vadali [7] discovered that a time delay filter which cancels the underdamped poles of the system results in the same control profile as the aforementioned input shaping filter. They also illustrated that the use of a series of time-delay filters, which have been designed for the nominal system frequency, results in increased robustness to modeling uncertainties. The witnessed robustness stems from additional zeros of the time delay filter being placed atop the system poles.

Other robustification methods include approaches such as designing input prefilters that maximize the uncertain region where residual vibration is less than a prespecified quantity. These are called Extra-Insensitive shapers [8]. They are characterized by the fact that the amount of residual vibration is fixed to zero at some points in the vicinity of the nominal system values.

Recently, Singh [9] proposed a minimax formulation to desensitize the controller with respect to modeling errors. The maximum magnitude of the residual energy over the entire uncertain space is minimized. A weighting function can also be incorporated taking the statistics of the model uncertainties into account.

This paper presents a near-minimax robustification method. The cost function is chosen as the magnitude of the frequency spectrum of the time-delay filter evaluated over the entire uncertain interval. By employing justificable approximations in the problem formulation, it is possible to derive analytical expressions relating the position of the zeros placed by the time delay filter to parameters describing the uncertain region. The performance of the resulting controller is comparable to that of a numerically optimized controller provided that the parameter deviation is reasonably small.

First, the problem is formulated and the minimax cost function is simplified. In the subsequent sections, different distributions of zeros will be analyzed. Controllers placing two or three zeros in the uncertain interval will be analyzed. The uncertain interval may or may not be symmetric with respect to the nominal value and the user can decide whether to place a zero of the time-delay filter at the nominal value or not. This is followed by a section giving numerical examples. The performance of the approximated and the real minimax controller are compared for a spring-mass system.

2 Problem Formulation

The paper is concerned with the design of near-minimax robust prefilters for undamped single input systems, which can be described by the differential equation

$$\ddot{y}(t) + \omega^2(p)\, y(t) = \omega^2(p)\, u(t). \tag{1}$$

ω denotes the frequency of the flexible mode and is subject to a parametric uncertainty. The uncertain space is spanned by p, known to be bounded by

$$p_{lb} \leq p \leq p_{ub}. \tag{2}$$

The nominal case is denoted as p_{nom}. The uncertain space does not need to be symmetric with regard to p_{nom}.

The cost function chosen is the magnitude of the time delay filter transfer function, evaluated over the entire uncertain space. The magnitude of the transfer function is a measure of how much a certain flexible mode will be excited by a given control sequence. Reducing the magnitude will reduce the amount of excitation of the associated flexible mode and thus the amount of residual vibration. Robustification is achieved by minimizing the maximum magnitude of the transfer function over the entire uncertain space. In addition, the magnitude may be forced to zero at p_{nom}. This ensures that the control performance reaches an optimum if all parameters assume their nominal values.

The cost function at every single point of the uncertain space is given as

$$F(p,x) = |G\left(j\omega(p), x\right)|. \tag{3}$$

The minimax robustification problem is then stated as

$$\min_x \max_p F(p,x). \tag{4}$$

This problem statement can be solved by employing a numerical optimization scheme. In the following, methods will be derived, which allow the design of controllers without solving the numerical optimization problem, thus simplifying the design process and reducing the amount of computational expense.

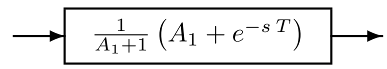

Figure 1: Structure of the Time Delay Filter Described by Eq. 5

3 Simplification of the Cost Function

A one delay time-delay filter as described by Singh [7] is given as

$$G(s) = \frac{1}{A_1+1}\left(A_1 + e^{-sT}\right). \tag{5}$$

The time delay filter is shown in Fig. 1. The magnitude of its transfer function is given by

$$\begin{aligned} &|G(\sigma + j\omega)| \\ &= \frac{\sqrt{\left(A_1 + e^{-\sigma T}\cos(\omega T)\right)^2 + \left(e^{-\sigma T}\sin(\omega T)\right)^2}}{A_1+1} \\ &= \frac{\sqrt{A_1^2 + 2\,A_1\,e^{-\sigma T}\cos(\omega T) + e^{-2\sigma T}}}{A_1+1}. \end{aligned} \tag{6}$$

For the following development, it is assumed that the structure has no damping. For this case, $\sigma = 0$ and $A_1 = 1$. The magnitude can then be written as

$$\begin{aligned} |G(j\omega)| &= \frac{1}{2}\sqrt{\left(1+\cos(\omega T)\right)^2 + \left(\sin(\omega T)\right)^2} \\ &= \frac{1}{2}\sqrt{2 + 2\,\cos(\omega T)}. \end{aligned} \tag{7}$$

The zeros of the time-delay filter are placed at the positions

$$s = j\frac{(2n+1)\pi}{T}\ \forall\ n = -\infty, \ldots, \infty. \tag{8}$$

The cosine is first split up using a trigonometric identity and then approximated by a Taylor Series Expansion around the zero located at ω_0.

$$\begin{aligned} &|G(j\omega)| \\ &= \frac{\sqrt{2 + 2\,\cos\left(\left(\omega_0 + \Delta\omega\right)T\right)}}{2} \\ &= \frac{\sqrt{2 + 2(-1)\,\left(1 - \frac{1}{2!}(\Delta\omega\,T)^2 + \frac{1}{4!}(\Delta\omega\,T)^4 - \ldots\right)}}{2} \\ &\approx \frac{\sqrt{(\Delta\omega\,T)^2}}{2} = \frac{1}{2}\Delta\omega\,T \end{aligned} \tag{9}$$

This shows that a purely linear relation between ω and $|G(j\omega)|$ may be used in the vicinity of a zero of the time-delay filter transfer function.

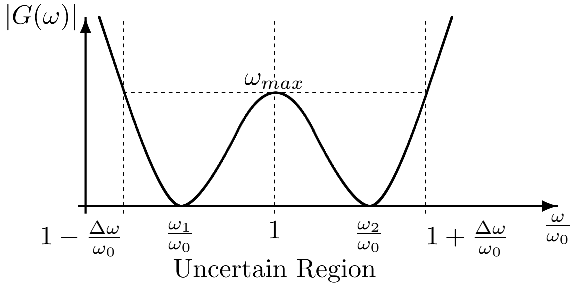

Figure 2: Magnitude of the Transfer Function of the Two Zero Minimax Robust Controller

This result will now be applied to time-delay filters placing more than one zero in the vicinity of a system pole. These time-delay filters can be written as a multiplication of individual time delay filters given by Eq. 5. For such a combination, the cost function can be approximated by a multiplication of terms as given in Eq. 9. This step is based on the assumption that the zeros of all time-delay filters are placed sufficiently close to each other. For the following developments, all frequencies are normalized with respect to ω_0, which will be the nominal frequency. This ensures that the entire development is independent of the location of nominal parameter values.

3.1 Two Zeros in the Uncertain Interval

In the following, the calculation of a two-zero minimax robust controller will be carried out. The two zeros will be located at $\frac{\omega_1}{\omega_0}$ and $\frac{\omega_2}{\omega_0}$. The uncertain interval is bounded by

$$1-\frac{\Delta\omega}{\omega_0} \le \frac{\omega}{\omega_0} \le 1+\frac{\Delta\omega}{\omega_0}. \tag{10}$$

Since the magnitude of the time-delay filter is not constrained at the nominal value, it can be assumed without a loss of generality that the nominal value is always the mid-point of the interval.

Figure 2 shows the general shape of the magnitude of the time delay filter transfer function. In order to find the minimum of all maximum values, the position of all possible maximal points along with their values must first be determined. Maximum values can be located at the left and/or right end of the uncertain interval as well as somewhere between these two endpoints.

The approximated cost function is given by

$$F(\omega) = |\omega-\omega_1|\,|\omega-\omega_2|, \tag{11}$$

The location of maxima within the uncertain interval must be determined. The position of the only maximum within the interval is given as

$$\frac{\omega_{max}}{\omega_0} = \frac{\omega_1+\omega_2}{2\,\omega_0}. \tag{12}$$

It has been shown that there are three candidate maximum values. One or more of these points will be maximum values of the cost function, depending on $\frac{\omega_1}{\omega_0}$ and $\frac{\omega_2}{\omega_0}$. The maximum is located at the left end of the interval, if

$$\begin{aligned} F(\omega_0-\Delta\omega) &\ge F(\omega_{max}) \\ F(\omega_0-\Delta\omega) &\ge F(\omega_0+\Delta\omega), \end{aligned} \tag{13}$$

which can be rewritten as

$$\begin{aligned} &\omega_0^2\left(\frac{\omega_1}{\omega_0}-\left(1-\frac{\Delta\omega}{\omega_0}\right)\right)\left(\frac{\omega_2}{\omega_0}-\left(1-\frac{\Delta\omega}{\omega_0}\right)\right) \\ &\ge \omega_0^2\left(\frac{\omega_{max}}{\omega_0}-\frac{\omega_1}{\omega_0}\right)\left(\frac{\omega_2}{\omega_0}-\frac{\omega_{max}}{\omega_0}\right), \\ &\omega_0^2\left(\frac{\omega_1}{\omega_0}-\left(1-\frac{\Delta\omega}{\omega_0}\right)\right)\left(\frac{\omega_2}{\omega_0}-\left(1-\frac{\Delta\omega}{\omega_0}\right)\right) \\ &\ge \omega_0^2\left(\left(1+\frac{\Delta\omega}{\omega_0}\right)-\frac{\omega_1}{\omega_0}\right)\left(\left(1+\frac{\Delta\omega}{\omega_0}\right)-\frac{\omega_2}{\omega_0}\right) \end{aligned} \tag{14}$$

Provided that these two inequalities hold true, the maximum value is given by

$$F = (\omega_1-(\omega_0-\Delta\omega))\,(\omega_2-(\omega_0-\Delta\omega)) \tag{15}$$

and can be minimized by

$$\frac{\omega_1}{\omega_0},\ \frac{\omega_2}{\omega_0} \to \left(1-\frac{\Delta\omega}{\omega_0}\right) \tag{16}$$

A similar development can be used to find out when the maximum value will be located at the right end of the interval. The maximum is located there, if the inequalities

$$\begin{aligned} F(\omega_0+\Delta\omega) &\ge F(\omega_{max}) \\ F(\omega_0+\Delta\omega) &\ge F(\omega_0-\Delta\omega), \end{aligned} \tag{17}$$

hold true. These constraints can be rewritten in a way similar to Eq. 14, which will not be shown here. The value at the right end of the interval,

$$F = ((\omega_0+\Delta\omega)-\omega_1)\,((\omega_0-\Delta\omega)-\omega_2)\,, \tag{18}$$

can be minimized by

$$\frac{\omega_1}{\omega_0},\ \frac{\omega_2}{\omega_0} \to \left(1+\frac{\Delta\omega}{\omega_0}\right) \tag{19}$$

A third case, which must be considered, is that the maximum is positioned at $\frac{\omega_{max}}{\omega_0}$. The inequalities for this case are given as

$$\begin{aligned} F(\omega_{max}) &\ge F(\omega_0-\Delta\omega) \\ F(\omega_{max}) &\ge F(\omega_0+\Delta\omega), \end{aligned} \tag{20}$$

This set of constraints can also be rewritten in the form given by Eq. 14, which will not be shown here. Provided that these two inequalities hold true, the cost function at this point evaluates to

$$F = (\omega_{max}-\omega_1)\,(\omega_2-\omega_{max}) \tag{21}$$

A reduction in the function value can be achieved by

$$\frac{\omega_1}{\omega_0}, \frac{\omega_2}{\omega_0} \rightarrow \frac{\omega_{max}}{\omega_0}. \tag{22}$$

The minimization requirements listed in Eq. 16, 19, and 22 contradict each other and cannot be pursued simultaneously. They will finally result in that all three possible maximum points assume an equal function value. The position of the poles, ω_1 and ω_2, can therefore be solved from the equations

$$\begin{aligned}
&\omega_0^2\left(\left(1+\frac{\Delta\omega}{\omega_0}\right)-\frac{\omega_1}{\omega_0}\right)\left(\left(1+\frac{\Delta\omega}{\omega_0}\right)-\frac{\omega_2}{\omega_0}\right)\\
&=\omega_0^2\left(\frac{\omega_1}{\omega_0}-\left(1-\frac{\Delta\omega}{\omega_0}\right)\right)\left(\frac{\omega_2}{\omega_0}-\left(1-\frac{\Delta\omega}{\omega_0}\right)\right),\\
&\omega_0^2\left(\left(1+\frac{\Delta\omega}{\omega_0}\right)-\frac{\omega_1}{\omega_0}\right)\left(\left(1+\frac{\Delta\omega}{\omega_0}\right)-\frac{\omega_2}{\omega_0}\right)\\
&=\omega_0^2\left(\frac{\omega_{max}}{\omega_0}-\frac{\omega_1}{\omega_0}\right)\left(\frac{\omega_2}{\omega_0}-\frac{\omega_{max}}{\omega_0}\right).
\end{aligned} \tag{23}$$

This set of constraints is solved by

$$\frac{\omega_1}{\omega_0}=1-\frac{1}{\sqrt{2}}\frac{\Delta\omega}{\omega_0}, \; \frac{\omega_2}{\omega_0}=1+\frac{1}{\sqrt{2}}\frac{\Delta\omega}{\omega_0}, \tag{24}$$

which represents the zero configuration for the minimax robust controller placing two zeros in the uncertain interval. The maximum values will be located at

$$\frac{\omega}{\omega_0}=1-\frac{\Delta\omega}{\omega_0}, \; \frac{\omega}{\omega_0}=1, \; \frac{\omega}{\omega_0}=1+\frac{\Delta\omega}{\omega_0}, \tag{25}$$

all of them yielding a cost function value of

$$F_{max}=\left(1-\frac{1}{\sqrt{2}}\right)\left(1+\frac{1}{\sqrt{2}}\right)\Delta\omega^2=\frac{1}{2}\Delta\omega^2 \tag{26}$$

3.2 Three Zeros in the Uncertain Interval

For many applications, the system parameters will most likely assume their nominal values. For those applications, it is desirable to achieve excellent control performance at the nominal point in the uncertain space. The best performance is achieved at those points in the uncertain space where the time delay filter transfer function is zero. Therefore, we will now require that a zero is placed at the nominal frequency $\frac{\omega}{\omega_0}=1$.

The filter presented in the previous section did not give the designer the opportunity to place a zero arbitrarily. A third zero will now be introduced, which can be placed arbitrarily. The general shape of the magnitude of the filter is shown in Fig. 3. As can already be seen from the figure, there are four candidate points for the maximum. The left and the right endpoint as well as two points within the uncertain interval.

For the first part of this section, it will be assumed that the uncertain interval is symmetric with respect to the nominal value ω_0, i. e. $\frac{\Delta\omega_1}{\omega_0}=\frac{\Delta\omega_2}{\omega_0}=\frac{\Delta\omega}{\omega_0}$. By formulating sets of inequality expressions as carried out in the previous section, it is possible to solve for the location of the poles in terms of the width of the uncertain interval. After going through the entire development, the zero configuration can be derived as

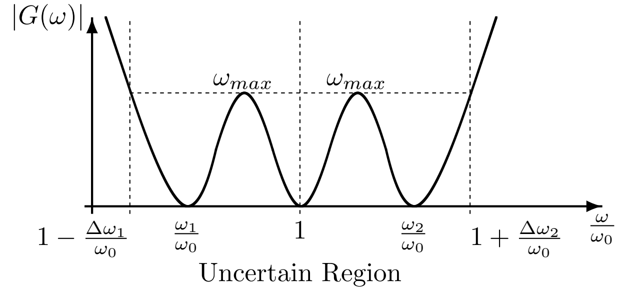

Figure 3: Magnitude of the Transfer Function of the Three-Zero Minimax Robust Controller

$$\frac{\omega_1}{\omega_0}=1-\frac{\sqrt{3}}{2}\frac{\Delta\omega}{\omega_0}, \; \frac{\omega_2}{\omega_0}=1, \; \frac{\omega_3}{\omega_0}=1+\frac{\sqrt{3}}{2}\frac{\Delta\omega}{\omega_0}. \tag{27}$$

The maximum values of the cost function will be located at

$$\begin{aligned}
\frac{\omega}{\omega_0}&=1-\frac{\Delta\omega}{\omega_0}\\
\frac{\omega}{\omega_0}&=1-\frac{1}{2}\frac{\Delta\omega}{\omega_0}\\
\frac{\omega}{\omega_0}&=1+\frac{1}{2}\frac{\Delta\omega}{\omega_0}\\
\frac{\omega}{\omega_0}&=1+\frac{\Delta\omega}{\omega_0}.
\end{aligned} \tag{28}$$

The cost function at these points is given by

$$F_{max}=\left(1-\frac{1}{2}\sqrt{3}\right)\left(1+\frac{1}{2}\sqrt{3}\right)\Delta\omega^2=\frac{1}{4}\Delta\omega^2 \tag{29}$$

Now, the assumption that the uncertain interval has symmetric bounds is abandoned. For this development, the bounds are denoted as

$$\begin{aligned}
\Omega_1&=1-\frac{\Delta\omega_1}{\omega_0}\\
\Omega_2&=1+\frac{\Delta\omega_2}{\omega_0}.
\end{aligned} \tag{30}$$

Two cases must be distinguished depending on the bounds of the uncertain interval. The first case under investigation deals with an uncertain interval for which the distance from the nominal point to the left border of the interval is larger than the distance to the right border, i. e. $\Delta\omega_1>\Delta\omega_2$. Going through the mathematical development leaves the designer with the implicit equations

$$\begin{aligned}&\left(\Omega_1^2-2\Omega_1\Omega_2+\Omega_2^2\right)x^4\\&+\left(-2\Omega_2^3-2\Omega_2\Omega_1^2+4\Omega_1^3\right)x^3\\&+\left(6\Omega_1\Omega_2^3+6\Omega_1^4+\Omega_2^4+3\Omega_1^2\Omega_2^2\right)x^2\\&+\left(-2\Omega_2\Omega_1^4+2\Omega_1^2\Omega_2^3-4\Omega_1\Omega_2^4+4\Omega_1^5\right)x\\&+\left(-4\Omega_1^3\Omega_2^3-3\Omega_1^4\Omega_2^2+\Omega_1^6-2\Omega_1^5\Omega_2-4\Omega_1^2\Omega_2^2\right)=0,\end{aligned}\tag{31}$$

and

$$\begin{aligned}&\left(\Omega_1^2+2\Omega_1\Omega_2-\Omega_2^2\right)x^2\\&+\left(\Omega_1^3-3\Omega_1\Omega_2^2+2\Omega_2^3\right)x\\&+\left(-2\Omega_1^3\Omega_2-3\Omega_1^2\Omega_2^2-\Omega_2^4\right)=0,\end{aligned}\tag{32}$$

which must be solved for x.

Comment on solutions The solution x relates to the zeros as

$$\begin{aligned}\frac{\omega_1}{\omega_0}&=1-\frac{\Omega_1^2\,x+\Omega_1^3-\Omega_2^3+\Omega_2^2\,x}{\Omega_1\,x+\Omega_1^2+\Omega_2^2-\Omega_2\,x}\\\frac{\omega_2}{\omega_0}&=1+x.\end{aligned}\tag{33}$$

From this set of equations, criteria can be found to select the right solution x from the solution vector. The solution must be real and must lie within the interval $0 \le x \le \Delta\omega_2$.

If the right interval is larger than the left interval, two extra steps have to be taken. First the problem is transformed so that the length of the left and the right uncertain interval are exchanged. The problem has thus been converted to the case treated previously. After the distance of the poles from the nominal values have been calculated, they are exchanged again.

4 Calculation of the Time-Delay Filter

Once the position of the zeros has been obtained, a time-delay filter can be set up which realizes these zeros. Depending on how much resources can be used, one can either calculate a time-optimal control profile or use a time-delay filter with fixed sampling time. For the latter, a pseudo inverse can be used to calculate the time delay filter profile, thus the time-delay filter design can be carried out in real-time. The time delay filter with $n-1$ delays and sampling time T is given as

$$G(s)=\sum_{i=0}^{n}A_i e^{-i\,s\,T}\tag{34}$$

The requirements to cancel a single pole at $s=j\,\omega$ can be written as

$$\begin{bmatrix}\sum_{i=0}^{n}A_i\cos(\omega\,i\,T)=0\\\sum_{i=0}^{n}A_i\sin(\omega\,i\,T)=0\end{bmatrix}\tag{35}$$

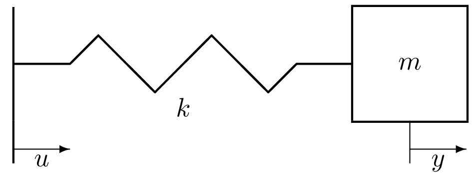

Figure 4: Spring Mass System

This equation can be written in vector form as

$$\begin{bmatrix}1, & \cos(\omega\,T), & \cos(2\omega\,T)\\0, & \sin(\omega\,T), & \sin(2\omega\,T)\end{bmatrix}\begin{bmatrix}A_0\\A_1\\A_2\end{bmatrix}=\begin{bmatrix}0\\0\end{bmatrix}.\tag{36}$$

This set of equations is of the form

$$A\,x=b\tag{37}$$

and can be solved by calculating the pseudo inverse of A given as

$$x=A^{\dagger}\,b,\tag{38}$$

where $\dagger$ denotes the pseudo-inverse.

5 Numerical Results

In this section, a comparison is carried out between the different robustification methods. The method is tested on a spring-mass system. The system under consideration is shown in Fig. 4. The dynamics of this system are given as

$$\ddot{y}(t)+\omega^2\,y(t)=\omega^2\,u(t),\tag{39}$$

where ω denotes the natural frequency. The natural frequency is assumed to be known only within a certain interval which is bounded by

$$1-\frac{\Delta\omega_1}{\omega_0}\le\frac{\omega}{\omega_0}\le 1+\frac{\Delta\omega_2}{\omega_0}.\tag{40}$$

The nominal value is given as $\frac{\omega}{\omega_0}=1$.

5.1 Two Zeros in the Uncertain Interval

In this section, different filters are compared. All filters may place two zeros in the uncertain interval. The location of the zeros has been compared for varying distances of the uncertain interval.

Figure 5 plots the magnitude of the transfer function over the natural frequency for an uncertain interval bounded by $0.8 \le \frac{\omega}{\omega_0} \le 1.2$. The uncertain interval is shaded in grey. This diagram shows the difference in sensitivity with respect to the natural frequency for the different controllers. The first controller shown in this diagram was designed to place both zeros at the mid-point of the uncertain interval. This is the standard robustification method if a pure pole cancellation approach is chosen. The zeros are locatec at

$$\frac{\omega_1}{\omega_0} = 1, \ \frac{\omega_2}{\omega_0} = 1 \tag{41}$$

The second controller was designed based on a minimax optimization approach using a numerical optimization package. The zeros have been placed at

$$\frac{\omega_1}{\omega_0} = 0.8591, \ \frac{\omega_2}{\omega_0} = 1.1395 \tag{42}$$

The third controller was designed using the technique described in this paper, which results in zeros being placed at

$$\frac{\omega_1}{\omega_0} = 0.8586, \ \frac{\omega_2}{\omega_0} = 1.1414 \tag{43}$$

As can be seen from the diagram, the difference between the minimax controller and the near minimax robust controller is very small. The error introduced by the assumptions is far less than one percent.

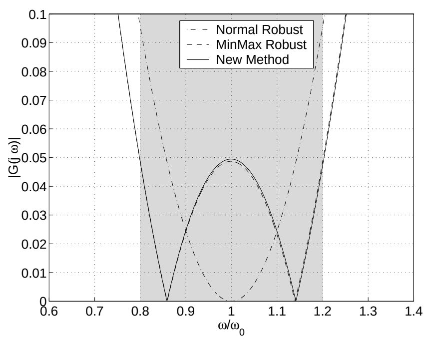

Figure 5: Cost Function over Parameter Deviation

The variation of the zeros over the width of the uncertain space is shown in Fig. 6. The grey shaded area denotes the uncertain interval. This diagram clearly illustrates that the position of the zeros can be approximated over a wide range of bounds of the uncertain space.

5.2 Three Zeros in the Uncertain Interval

Two different cases can be distinguished, depending on whether the uncertain interval is symmetric with respect to the nominal value or not. First, a symmetric uncertainty is assumed. The nominal value is given as $\frac{\omega}{\omega_0} = 1$ and ω is bounded by $0.8 \leq \frac{\omega}{\omega_0} \leq 1.2$. Different controllers have been designed for this system. A plot of the cost function over parameter deviation for the different controllers is shown in Fig. 7. The controller design employing the pole cancellation technique places all three poles at

$$\frac{\omega_1}{\omega_0} = 1, \ \frac{\omega_2}{\omega_0} = 1, \ \frac{\omega_3}{\omega_0} = 1. \tag{44}$$

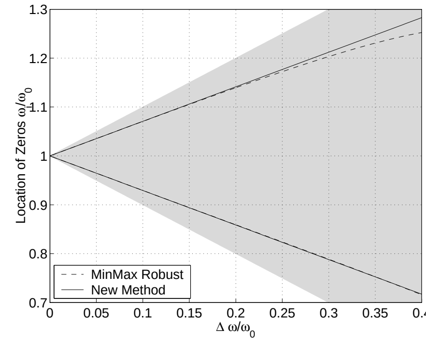

Figure 6: Variation of Zeros over Uncertainty

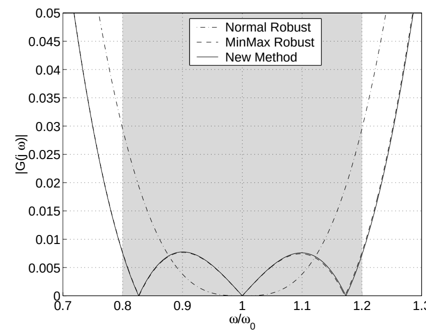

Figure 7: Cost Function over Parameter Deviation

The minimax robust controller, which was constrained to place at least one zero at $\frac{\omega}{\omega_0} = 1$, has three zeros in the uncertain interval, located at

$$\frac{\omega_1}{\omega_0} = 0.8273, \ \frac{\omega_2}{\omega_0} = 1, \ \frac{\omega_3}{\omega_0} = 1.1716. \tag{45}$$

The controller which was designed utilizing the approximation technique places the zeros at

$$\frac{\omega_1}{\omega_0} = 0.8268, \ \frac{\omega_2}{\omega_0} = 1, \ \frac{\omega_3}{\omega_0} = 1.1732. \tag{46}$$

The variation of the zeros over the width of the uncertain range is illustrated in Fig.8. The error introduced by the approximation is again less than one percent.

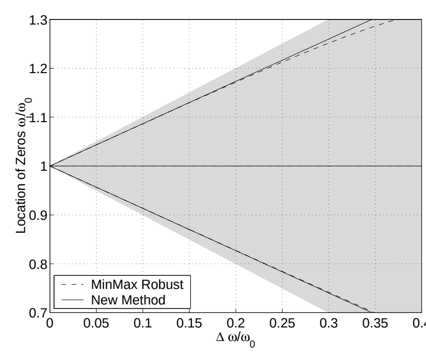

Figure 8: Variation of Zeros over Uncertainty

In the following, the assumption concerning symmetry of the uncertain interval with regard to the nominal point is abolished. The nominal value is still placed at $\frac{\omega}{\omega_0} = 1$, whereas the natural frequency is bounded by $0.75 \leq \frac{\omega}{\omega_0} \leq 1.15$.

The pole cancellation controller will again consist of three zeros placed at the nominal value, i. e.

$$\frac{\omega_1}{\omega_0} = 1,\ \frac{\omega_2}{\omega_0} = 1,\ \frac{\omega_3}{\omega_0} = 1. \tag{47}$$

The reference minimax design locates zeros of the time delay filter at

$$\frac{\omega_1}{\omega_0} = 0.7814,\ \frac{\omega_2}{\omega_0} = 1,\ \frac{\omega_3}{\omega_0} = 1.0987. \tag{48}$$

The near-minimax robust controller places its zeros in the close vicinity of the reference design at

$$\frac{\omega_1}{\omega_0} = 0.7807\ \frac{\omega_2}{\omega_0} = 1,\ \frac{\omega_3}{\omega_0} = 1.1014. \tag{49}$$

The mislocation of the poles caused by the approximations is far less than one percent. The magnitude of the transfer function as a function of frequency is shown in Fig.9.

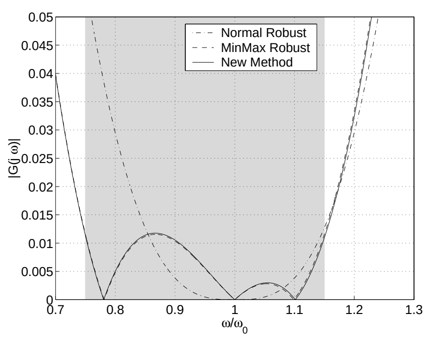

Figure 9: Cost Function over Parameter Deviation

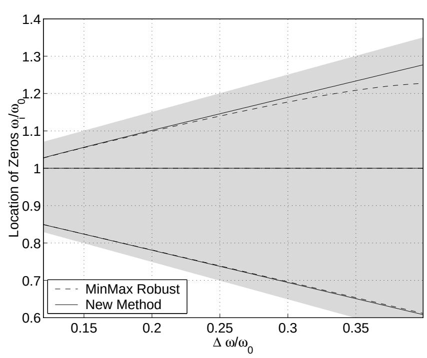

Figure 10: Variation of Zeros over Uncertainty

The next example shows the opposite case, where the interval is unevenly divided by the nominal value such that the bigger part of the interval is to the right of the nominal value. The nominal value is placed at $\frac{\omega}{\omega_0} = 1$, while the maximum parameter deviation is bounded by $0.85 \leq \frac{\omega}{\omega_0} \leq 1.25$. As in all previous examples, the pole cancellation controller will place all zeros at the nominal value, i. e.

$$\frac{\omega_1}{\omega_0} = 1,\ \frac{\omega_2}{\omega_0} = 1,\ \frac{\omega_3}{\omega_0} = 1. \tag{50}$$

For the reference minimax design, the zeros turned out to be at

$$\frac{\omega_1}{\omega_0} = 0.7814,\ \frac{\omega_2}{\omega_0} = 1,\ \frac{\omega_3}{\omega_0} = 1.0987. \tag{51}$$

The near-minimax robust controller places the zeros at

$$\frac{\omega_1}{\omega_0} = 0.7807\ \frac{\omega_2}{\omega_0} = 1,\ \frac{\omega_3}{\omega_0} = 1.1014. \tag{52}$$

The error caused by the assumptions is again far less than one percent. Figure 11 presents a magnitude plot of the different transfer functions of the time delay filters and Fig.12 shows the variation of the zeros as a function of the uncertain interval.

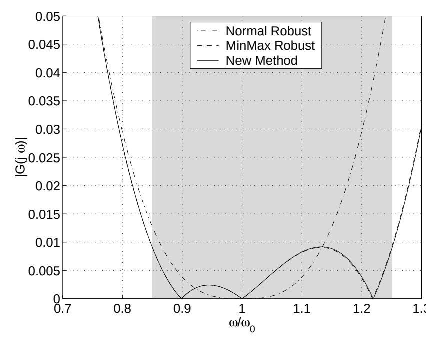

Figure 11: Cost Function over Parameter Deviation

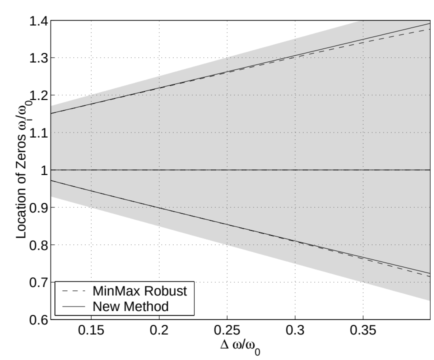

Figure 12: Variation of Zeros over Uncertainty

6 Conclusion

This paper presented the design of minimax robust time delay filters. The cost function chosen was the magnitude of the time delay filter transfer function evaluated over the entire uncertain space. The magnitude of the time delay filter transfer function, which is easy to calculate, approximately measures the amount of residual vibration. The smaller the magnitude of the transfer function at a certain point, the smaller the impact level. Robustness can be achieved by minimizing the maximum value over the entire uncertain space. A constraint can be added which forces the magnitude of the transfer function at the nominal values to zero.

A numerical optimization package can be used to solve the minimax problem. However, the computational expense of these methods is quite large and precludes realtime generation of the control profile. The paper presented a method which allows generation of near-minimax robust control profiles. The parameters of the time-delay filters are given as functions of the nominal frequency as well as the bounds of the uncertain space. These parameters can easily be obtained in real-time.

Numerical results have proven the feasibility of the proposed design method. The error introduced by the approximations is small for the cases presented in the section on numerical examples.

Acknowledgement

Part of this paper was completed during the second authors stay in Germany under the auspices of the Alexander von Humboldt Stiftung. The second author gratefully acknowledges the Humboldt-Stiftung for their support.

References

[1] Junkins J. L., Rahman, Z., & Bang, H. 1990. *Near-Minimum Time Maneuvers of Flexible Vehicles: A Liapunov Control Law Design Method, Mechanics and Control of Large Flexible Structures*. Washington, DC: AIAA Publication.

[2] Ballhaus, W.L., Rock, S.M. & Bryson, A.E. 1992. Optimal Control of a Two-Link Flexible Robotic Manipulator Using Time-Varying Controller Gains. *Amer. Astronautics Soc. paper 92-055*.

[3] Bhat, S. P., & Miu, D. K. 1991. Minimum Power and Minimum Jerk Control and its Application in Computer Disk Drives. *IEEE Transactions on Magnetics*, **27**(6), 4471-4475.

[4] Singhose, W. E., Porter, L. J., & Seering, W. P. 1997. Input Shaped Control of a Planar Gantry Crane with Hoisting. *1997 American Control Conference*. Albuquerque, NM.

[5] Smith, O. J. M. 1957. Posicast Control of Damped Oscillatory Systems. *Proceedings of the IRE*, 1249-1255.

[6] Singer, N. C., & Seering, W. P. 1990. Preshaping Command Inputs to Reduce System Vibrations. *ASME Journal of Dynamic Systems, Measurement and Control*, **115**, 76-82.

[7] Singh, T., & Vadali, S. R. 1995. Robust Time-Delay Control of Multimode Systems. *International Journal of Control*, **62**(6), 1319-1339.

[8] Singhose, W. E., Porter, L. J., & Singer, N. P. 1995. Vibration Reduction Using Multi-Hump Extra-Insensitive Input Shapers. *Proceedings of the American Control Conference*.

[9] Singh, T. 2001. Minimax Design of Robust Controllers for Flexible Structures. In review. To appear in *Journal of Guidance, Control and Dynamics*.